

# Active surge control of centrifugal compressors using drive torque

Jan Tommy Gravdahl\*, Olav Egeland\* and Svein Ove Vatland\*\*

\* Department of Engineering Cybernetics, NTNU, N-7491 Trondheim, Norway

\*\* ABB Corporate Research, Bergerveien 12, N-1375 Billingstad, Norway

## Abstract

A novel approach to active surge control is presented. A centrifugal compressor driven by an electrical motor is studied, and the *drive itself* is used for surge control, thus eliminating the need for additional actuators. It is shown that by using the rotational speed of the motor as control, previous unstable operating points to the left of the surge line can be made globally exponentially stable. It is also shown that using the torque of the drive as control ensures exponential convergence. The proposed method is simulated on a compressor model using an approximation of a real compression system.

## 1 Background

Surge is an unstable operation mode of centrifugal compressors, which occurs when the operating point of the compressor is located to the left of the surge line, which is the stability limit in the compressor map. The phenomenon is manifested as oscillations of the mass flow, pressure rise and rotational speed of the compressor. Surge is highly undesired, and can cause severe damage to the machine. Traditionally, surge has been avoided using a surge avoidance scheme. Such schemes use various measures to keep the operating point of the compressor away from the surge line. Typically, a surge control line is drawn at a distance from the surge line, and the surge avoidance scheme ensures that the operating point does not cross this line. This method restricts the operating range of the machine, and efficiency is limited. Usually a recycle line around the compressor is used as actuation. Active surge control is fundamentally different to surge avoidance in that the unstable phenomenon is sought to be stabilized instead of avoided. Thus the operating regime of the compressor is enlarged.

Active surge control of compressors was first introduced by [1], and since then a number of results have been published. Different actuators have been used, and examples include recycle, bleed and throttle valves, gas injection, variable guide vanes and a number of others. For an overview, consult [2] or [3]. In this work we propose to use the electrical drive of the compressor as a means of active surge control, as depicted in Figure 1. The advantage of this is that the drive is already present, and no additional actuation device is required. This means that the compressor can be operated at a low flow without recycling, and there is a potential for reduced energy consumption of the compressor.

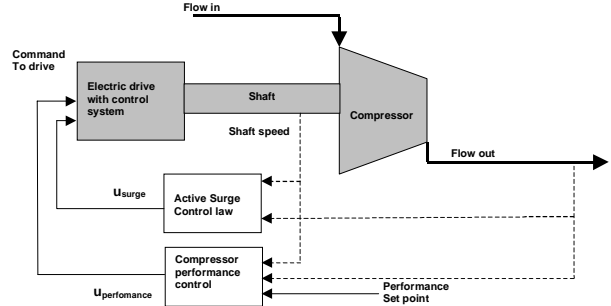


**Figure 1:** The compression system considered consists of a centrifugal compressor driven by an electrical motor.

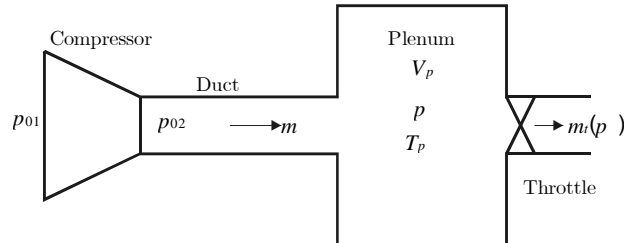


**Figure 2:** The compressor, plenum, throttle system of [4]

## 2 Model

### 2.1 Dynamics

A classical result in the field of compressor surge modeling is the model of Greitzer [4] who modelled a basic compression system consisting of a compressor, a plenum volume, a throttle valve and in-between ducting as shown in Figure 2. In order to study the drive torque as control variable for surge control, we need a model that takes variable speed into account. In [5], the Greitzer-model was further developed, and rotational speed was included as a state in the model. A similar model was derived in [6], using an approach based on energy based analysis. Experimental results confirming the model of [6] were presented in [7] and [8]. In this paper we will employ the compressor model derived in [6]. The model is derived by calculating the mass balance of the plenum volume, integrating the one dimensional Euler equation (the momentum balance) over the length of the exit duct, and calculating the torque bal-

ance of the rotating shaft. The model is written

$$\dot{p} = \frac{a_{01}^2}{V_p}(m - m_t) \quad (1)$$

$$\dot{m} = \frac{A_1}{L_c}(\Psi_c(m, \omega)p_{01} - p) \quad (2)$$

$$\dot{\omega} = \frac{1}{J}(\tau_d - \tau_c), \quad (3)$$

where  $p$  is the plenum pressure,  $m$  is the compressor mass flow,  $\omega$  is the rotational velocity of the shaft,  $\Psi_c(m, \omega)$  is the compressor characteristic,  $m_t$  is the throttle flow,  $A_1$  is the throughflow area,  $L_c$  is the duct length,  $V_p$  is the plenum volume,  $p_{01}$  is the ambient pressure,  $a_{01}$  is the sonic velocity at ambient conditions,  $J$  is the inertia of all rotating parts, and  $\tau_d$  and  $\tau_c$  is the drive torque and compressor load torque, respectively. The throttle flow is given by

$$m_t = k_t \sqrt{p - p_{01}},$$

where  $k_t > 0$  is a parameter proportional to throttle opening. The compressor torque  $\tau_c$  is calculated as

$$\tau_c = |m| r_2 \sigma U_2, \quad (4)$$

where  $r_2$  is the impeller diameter,  $\sigma$  is the slip factor and  $U_2$  is the impeller tip speed. The drive torque  $\tau_d$  will be used as the control variable. For a detailed derivation of the model, consult [6] and [8]. We will study the dynamics around an equilibrium point. The equilibrium values are denoted by  $(\cdot)_0$ , while deviations from the equilibrium are denoted by  $(\hat{\cdot})$ . The deviations from the equilibrium are written

$$\begin{aligned} \hat{m} &= m - m_0, \quad \hat{p} = p - p_0, \quad \hat{\omega} = \omega - \omega_0 \\ \hat{m}_t &= m_t - m_{t0}, \quad \hat{\Psi}_c = \Psi_c - \Psi_{c0} \end{aligned}$$

where the equilibrium values must satisfy  $m_0 = m_{t0}$  and  $p_0 = \Psi_{c0}$ . The model (1)-(3) in new coordinates  $(\hat{\cdot})$  is written

$$\begin{aligned} \dot{\hat{p}} &= \frac{a_{01}^2}{V_p}(\hat{m} - \hat{m}_t) \\ \dot{\hat{m}} &= \frac{A_1}{L_c}(\hat{\Psi}_c p_{01} - \hat{p}), \\ \dot{\hat{\omega}} &= \frac{1}{J}(\hat{\tau}_d - \hat{\tau}_c), \end{aligned} \quad (5)$$

while the dynamics of the plenum pressure and the mass flow only are written

$$\begin{aligned} \dot{\hat{p}} &= \frac{a_{01}^2}{V_p}(\hat{m} - \hat{m}_t) \\ \dot{\hat{m}} &= \frac{A_1}{L_c}(\hat{\Psi}_c p_{01} - \hat{p}) \end{aligned} \quad (6)$$

For controller design we will assume that control variable is the angular velocity  $\omega$  of the compressor shaft. Then later we will study the effect of the fact that the control variable is the electrical motor torque  $\tau_d$ , while  $\omega$  is controlled by an internal high gain loop.

## 2.2 Compressor map

**2.2.1 Introduction:** In order to simulate the response of the compression system, a measured compressor map from a real centrifugal compressor will be used. A number of operating points on each measured constant speed line will be used to calculate a third order polynomial approximation to the speed lines. The third order polynomial is accepted in the literature (see e.g.[4]) as a suitable approximation of the speed lines. The zero-mass flow point will also be used in the calculations of the speed lines, and the third order form also gives the negative flow part of the characteristic.

**2.2.2 Calculation of the zero-mass-flow pressure rise:** Due to centrifugal effects, a centrifugal compressor will produce a pressure rise even at zero flow. This zero-mass-flow pressure rise can be found by studying the *rothalpy*  $I$ , which is a conserved quantity, [9]:

$$I = h + \frac{1}{2}W^2 - \frac{1}{2}U^2,$$

where  $h$  is specific enthalpy,  $W$  is relative speed between the fluid and the blades, and  $U$  is tangential impeller speed. Since the rothalpy  $I$  is unchanged between the inlet (subscript 1) and the outlet (subscript 2) of the impeller, we have that

$$\Delta h = h_2 - h_1 = \frac{1}{2}(U_2^2 - U_1^2) - \frac{1}{2}(W_2^2 - W_1^2),$$

where  $U_1$  and  $U_2$  are the tangential velocities at inlet and outlet, and  $W_1$  and  $W_2$  are the relative velocities between the moving fluid and the rotating blades at inlet and outlet. At zero mass flow, the relative velocities  $W_1$  and  $W_2$  vanish, and we have

$$\Delta h|_{m=0} = \frac{1}{2}(U_2^2 - U_1^2) = \frac{\pi^2 N^2}{2}(D_2^2 - D_1^2). \quad (7)$$

Assuming isentropic pressure rise,

$$\Psi_c(m, \omega) = \frac{p_{02}}{p_{01}} = \left(1 + \frac{\Delta h}{c_p T_{01}}\right)^{\frac{\kappa}{\kappa-1}}, \quad m > 0. \quad (8)$$

holds, for details see [8], and by combining (7) and (8), we get at zero mass flow

$$\Psi_c(0, N) = \Psi_o = \left(1 + \frac{\pi^2 N^2 (D_2^2 - D_1^2)}{2c_p T_{01}}\right)^{\frac{\kappa}{\kappa-1}}, \quad (9)$$

where  $N = 2\pi\omega$  is the rotational speed in rounds per second. The zero-flow-pressure rise has been calculated using (9) for five different speeds. These values, as well as three points on each measured speed line (shown as circles) are shown in Figure 3.

**2.2.3 Polynomial approximation of compressor map:** Also shown in Figure 3 are the third order polynomial approximations of the speed lines at five different speeds. The approximations are calculated using the MATLAB function `polyfit`, and for the five chosen speed lines, results are:

$$\begin{aligned} \Psi_c(m, 300) &= 1.602 - 0.063m + 0.167m^2 - 0.044m^3, \\ \Psi_c(m, 340) &= 1.829 - 0.097m + 0.183m^2 - 0.030m^3, \\ \Psi_c(m, 400) &= 2.251 - 0.144m + 0.191m^2 - 0.024m^3, \\ \Psi_c(m, 460) &= 2.809 - 0.166m + 0.178m^2 - 0.018m^3, \\ \Psi_c(m, 500) &= 3.270 - 0.205m + 0.174m^2 - 0.015m^3. \end{aligned}$$

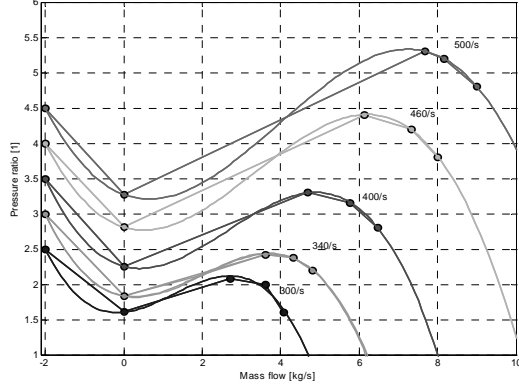


**Figure 3:** The measured speed lines (solid lines) and the polynomial approximations (dashed lines).

A compressor map is also continuous in the rotational speed, so in order to simulate the system, there is a need for making the approximated map also continuous in rotational speed. For this reason, the coefficients of the third order polynomials in are chosen to be functions of rotational speed. The polynomial approximation for each speed line can be written as

$$\Psi_c(m, N) = c_0(N) + c_1(N)m + c_2(N)m^2 + c_3(N)m^3,$$

where the functions

$$c_i(N) = c_{i0} + c_{i1}N + c_{i2}N^2 + c_{i3}N^3$$

are calculated by using polynomial approximation yet again. This approach was also taken by [10], using second order polynomials  $c_i(N) = c_{i0} + c_{i1}N + c_{i2}N^2$ . However, in our case it is necessary to use third order polynomials. This comes clear when inspecting Figure 4, where the polynomial coefficients of the five polynomials are plotted as a function of rotational speed. As can be seen, a fairly good fit can be made with third order. For  $c_0(N)$ , the zero-mass-flow pressure rise, it is seen from the figure that a linear approximation is sufficient. The resulting approximated compressor map which will be used in simulations is shown in Figure 5.

### 3 Controller design

#### 3.1 Surge control

The new feature of the proposed method is that we let the shaft velocity  $\hat{\omega}$  be a function of the mass flow  $\hat{m}$ , thereby ensuring that the compressor can be operated to the left of the surge line without going into surge. We first assume that the shaft speed  $\omega$  is our input control variable, and we will later consider the case that instead the drive torque  $\tau_d$  is the control. The following theorem can now be stated:

**Theorem 1** *The control law*

$$\hat{\omega} = -c\hat{m}, \quad (10)$$

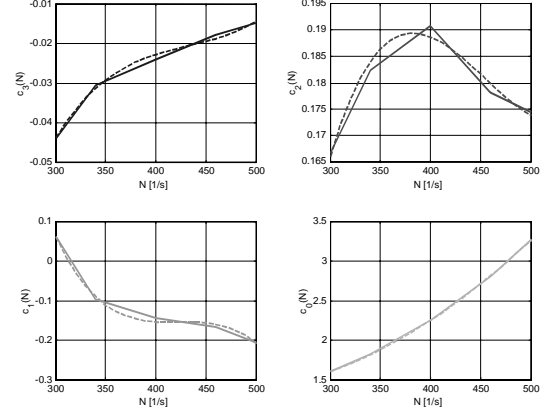


**Figure 4:** The coefficients  $c_i$  as functions of speed  $N$  (solid lines), and their polynomial approximations (dashed lines).

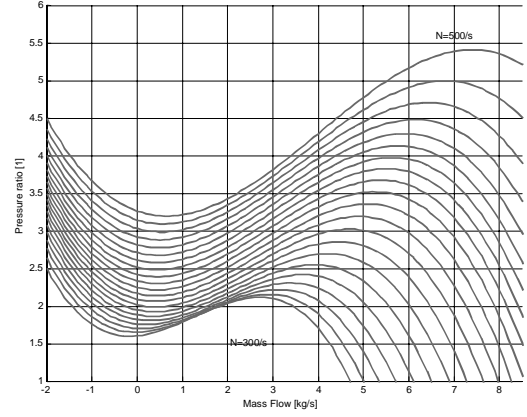


**Figure 5:** The approximated compressor map.

where the gain  $c$  is chosen according to

$$c > \frac{\partial \hat{\Psi}_c / \partial \hat{m}}{\partial \hat{\Psi}_c / \partial \hat{\omega}} \quad (11)$$

makes the origin of (6) globally exponentially stable.

**Proof:** Consider the Lyapunov function candidate

$$V = \frac{V_p}{a_{01}} \hat{p}^2 + \frac{L}{A} \hat{m} > 0, \forall (\hat{m}, \hat{p}) \neq (0, 0) \quad (12)$$

The time derivative along the solutions of the nonlinear system (6) is

$$\begin{aligned} \dot{V} &= \frac{a_{01}^2}{V_p} \hat{p} \dot{\hat{p}} + \frac{L}{A} \hat{m} \dot{\hat{m}} = \hat{p}(\hat{m} - \hat{m}_t) + \hat{m} (\hat{\Psi}_c p_{01} - \hat{p}) \\ &= \dot{V}_1 + \dot{V}_2 = -\hat{p} \hat{m}_t(\hat{p}, p_0) + \hat{m} \hat{\Psi}_c(\hat{m}, \hat{\omega}) p_{01} \end{aligned} \quad (13)$$

The throttle, or load, is assumed to be passive in the sense that it consumes energy from the compressor, which implies

$$\dot{V}_1 = -\hat{p}\hat{m}_t(\hat{p}, p_0) < -k_p\hat{p}^2 < 0, \forall \hat{p} \neq 0 \quad (14)$$

for some  $k_p > 0$ , where  $k_p$  depends on the slope of the throttle characteristic. This is illustrated in Figure 6. In order to prove stability, we now have to show that  $\dot{V}_2 < 0$ . In open loop, the compressor characteristic  $\hat{\Psi}_c(\hat{m}, \hat{\omega})$  is monotonically increasing in  $\hat{m}$  for  $\hat{m} < 0$ , that is

$$\frac{\partial \hat{\Psi}_c(\hat{m}, \hat{\omega})}{\partial \hat{m}} > 0, \forall \hat{m} < 0.$$

This is illustrated in Figure 7. We now chose

$$\hat{\omega} = -c\hat{m}.$$

As  $\hat{\Psi}_c(\hat{m}, \hat{\omega})\big|_{\hat{m}=0} = 0$ , a sufficient condition for  $\hat{\Psi}_c(\hat{m}, -c\hat{m})$  to be located in the 2nd and 4th quadrant in the  $(\hat{m}, \hat{\Psi}_c)$ -coordinate system is that  $\hat{\Psi}_c(\hat{m}, \hat{\omega})\big|_{\hat{\omega}=-c\hat{m}}$  is monotonically *decreasing*, that is

$$\frac{d\hat{\Psi}_c(\hat{m}, \hat{\omega})}{d\hat{m}} = \frac{\partial \hat{\Psi}_c}{\partial \hat{m}} + \frac{\partial \hat{\Psi}_c}{\partial \hat{\omega}} \frac{\partial \hat{\omega}}{\partial \hat{m}} = \frac{\partial \hat{\Psi}_c}{\partial \hat{m}} - c \frac{\partial \hat{\Psi}_c}{\partial \hat{\omega}} < 0$$

which is satisfied provided  $c$  is chosen according to (11).

As  $\hat{\Psi}_c(\hat{m}, \hat{\omega})\big|_{\hat{\omega}=-c\hat{m}}$  now is monotonically decreasing and passing through the origin, that is located in the 1st and 3rd quadrants, we have that

$$\dot{V}_2 = \hat{m}\hat{\Psi}_c(\hat{m}, -c\hat{m})p_{01} < 0, \forall \hat{m} \neq 0. \quad (15)$$

Moreover,  $\dot{V}_2$  can always be bounded from above as

$$\dot{V}_2 = \hat{m}\hat{\Psi}_c(\hat{m}, -c\hat{m})p_{01} < -k_m\hat{m}^2, \forall \hat{m} \neq 0. \quad (16)$$

for a constant  $k_m > 0$ . From (16) it follows that

$$\hat{\Psi}_c(\hat{m}, -c\hat{m})p_{01} < -k_m\hat{m}, \quad \hat{m} > 0. \quad (17)$$

As  $\hat{\Psi}_c(\hat{m}, -c\hat{m})p_{01}$  is monotonically decreasing and passing through the origin,  $\hat{\Psi}_c(\hat{m}, -c\hat{m})p_{01}$  is also bounded from above by the tangent through the origin, that is

$$\hat{\Psi}_c(\hat{m}, -c\hat{m})p_{01} < p_{01} \frac{d\hat{\Psi}_c(\hat{m}, -c\hat{m})}{d\hat{m}} \hat{m}.$$

By choosing

$$k_m = -p_{01} \frac{d\hat{\Psi}_c(\hat{m}, -c\hat{m})}{d\hat{m}} \bigg|_{\hat{m}=0}$$

(17) and (16) follows. A similar argument can be made for the case  $\hat{m} < 0$ . By (14) and (16), we now have that

$$\dot{V} = \dot{V}_1 + \dot{V}_2 < -k_p\hat{p}^2 - k_m\hat{m}^2 < -kV, \forall (\hat{m}, \hat{p}) \neq (0, 0)$$

and the result follows.  $\blacksquare$

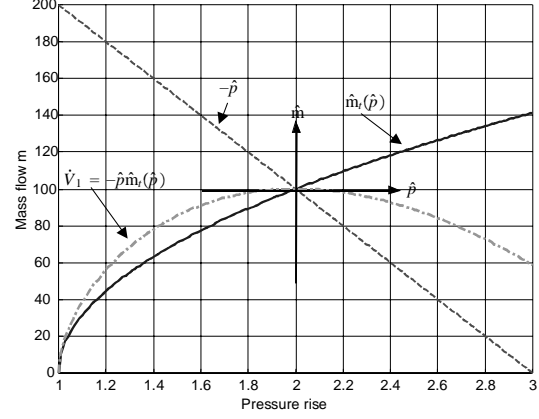


Figure 6: Calculation of  $\dot{V}_1$ .

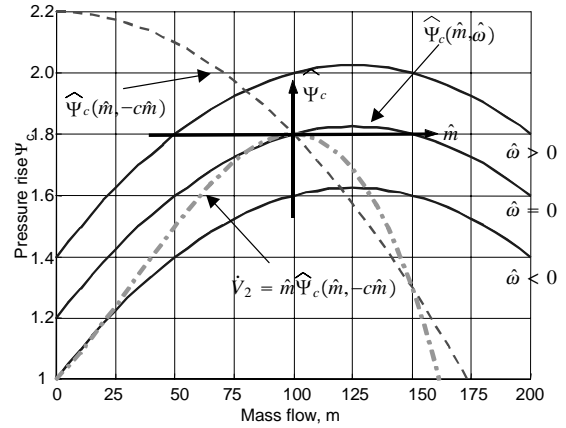


Figure 7: Calculation of  $\dot{V}_2$ .

It is seen from (10) that the gain  $c$  has a lower bound given by the ratio between the sensitivity of the characteristic  $\Psi_c$  with respect to the mass flow  $m$ , and the sensitivity of  $\Psi_c$  with respect to the shaft speed  $\omega$ . This result is related to another well known result in compressor control (see e.g. [11] or [6]): When using a close coupled valve (CCV) to stabilize a centrifugal compressor, the control law gain must be greater than the sensitivity of the characteristic  $\Psi_c$  with respect to the mass flow  $m$ . The CCV-approach aims at using the pressure drop over the valve to create a combined compressor and valve characteristic with negative slope in the equilibrium and thereby ensuring stability. The approach in this study achieves the same effect without imposing an unwanted pressure drop in the compression system. The proposed controller ensures that in closed loop the compressor characteristic has a negative slope in the equilibrium. This can be seen from the plot of  $\hat{\Psi}_c(\hat{m}, -c\hat{m})$  in Figure 7.

Also worth noticing is that, according to Chetaev's instability theorem, the equilibrium is unstable if the weaker sector nonlinearity (15) does not hold. This agrees with the well-known result that if  $\omega$  is kept con-

stant, that is  $\hat{\omega} = 0$ , then the compressor is unstable to the left of the surge line.

If we take the shaft dynamics (3) into consideration and follow the same procedure as in the proof of Theorem 1, the time derivative of the Lyapunov function candidate (12) along the trajectories of (6) is,

$$\dot{V} < -k_p \hat{p}^2 - k_m \hat{m}^2 + \hat{m} \delta(t), \quad (18)$$

where  $\delta = A/L\tilde{\Psi}_c$  and  $\tilde{\Psi}_c := \Psi_c(m, \omega) - \Psi_c(m, \omega_d)$  is the error in the compressor pressure  $\Psi_c$  due to the shaft dynamics related to the convergence of  $\omega$  to the desired value  $\omega_d = \omega_0 - c\hat{m}$ . It is seen that the system will converge exponentially towards the equilibrium whenever

$$k_m |\hat{m}| > |\delta(t)|. \quad (19)$$

Therefore, if the shaft dynamics are sufficiently fast so that  $\delta(t)$  converges quickly to zero, the system will converge to a small area around the equilibrium with exponential rate of convergence.

Disturbances may be treated in a similar way. Assume that there are disturbances to the system so the dynamics are

$$\begin{aligned} \dot{\hat{p}} &= \frac{a_{01}^2}{V_p} (\hat{m} - \hat{m}_t) + \delta_p \\ \dot{\hat{m}} &= \frac{A_1}{L_c} (\hat{\Psi}_c p_{01} - \hat{p}_p) + \delta_m \end{aligned} \quad (20)$$

Then the time derivative of the Lyapunov function candidate becomes

$$\dot{V} < -k_p \hat{p}^2 - k_m \hat{m}^2 + \hat{p} \delta_p + \hat{m} \delta_m,$$

which shows that  $V$  will decrease as long as

$$k_p \hat{p}^2 + k_m \hat{m}^2 > \hat{p} \delta_p + \hat{m} \delta_m.$$

In fact the state vector  $\hat{x} = (\hat{p} \ \hat{m})^T$  will converge exponentially to the region

$$\|\hat{x}\| < \beta := \frac{\max(\delta_p, \delta_m)}{\min(k_p, k_m)}.$$

Note that this is valid for all disturbances without any upper bound on  $(\delta_p, \delta_m)$ . The scalar  $k_p$  is given by the slope of the throttle characteristic, while  $k_m$  is given by the mass flow gain  $c$ . It is seen that  $\min(k_p, k_m)$  has an upper bound, which is  $k_p$ . It will make sense to select the gain  $c$  so that  $k_m$  is of the same magnitude as  $k_p$ . Satisfactory results will then be obtained provided that the disturbances  $(\delta_p, \delta_m)$  are sufficiently small so that  $\|\hat{x}\| < \beta$  gives acceptable operation of the compressor around the equilibrium. This depends on the disturbance specifications and the slope  $k_p$  of the throttle curve.

### 3.2 Velocity control

Let the electrical motor torque be generated by  $\tau_d = \hat{\tau} + \tau_0$  where  $\tau_0 = \tau_{c0}$  is the torque required in the equilibrium point, and  $\hat{\tau} = K_1(\omega_d - \omega)$  is the feedback control law that is used to obtain the desired shaft speed  $\omega_d = \omega_0 - c\hat{\omega}$ . The resulting control law is

$$\tau_d = -K_1 \hat{\omega} - K_2 \hat{m} + \tau_0$$

where the feedback gain for the mass flow is  $K_2 = K_1 c$ . In practical implementations we propose the use of integral action to generate the term  $\tau_0$ . The integral term  $-K_I \int \hat{\omega}(t') dt'$  is included in order to keep the compressor at the desired speed, and can be regarded as part of the performance control system, see Figure 1. This gives the control law

$$\tau = -K_1 \hat{\omega} - K_2 \hat{m} - K_I \int \hat{\omega}(t') dt'. \quad (21)$$

By using the analysis presented in equations (18) to (19), it can be concluded that applying a drive torque according to (21) ensures that the states of the system (5) converges exponentially to a small region around the origin.

## 4 Simulations

### 4.1 Surge

In this section it is illustrated that the model is capable of simulating surge, the instability which will be stabilized in the next section. Results are presented from simulations of the compressor system when it is driven into surge by a drop in mass flow. The compressor is initially operating in a stable operating point close to  $m \approx 5$  kg/s, when a throttle change induces a drop in mass flow of 20%, consequently driving the compressor over the surge line down to about  $m \approx 4$  kg/s, and ultimately ending up in a deep surge condition. The compressor response to this disturbance is shown in Figure 8. A constant drive torque is used. The compressor undergoes deep surge with oscillations in mass flow, pressure rise and shaft speed.

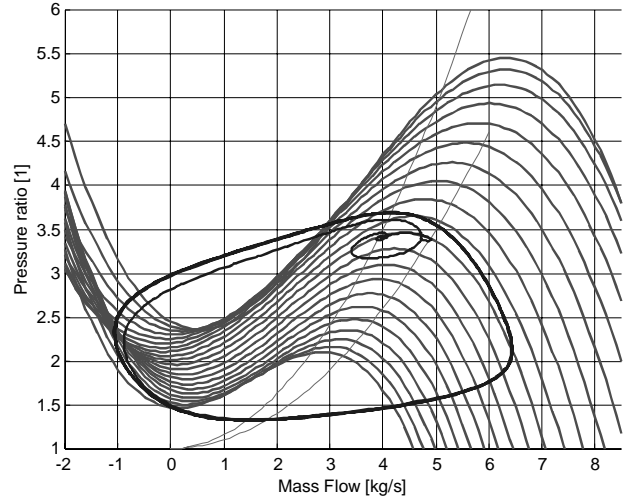


**Figure 8:** Compressor response when the operating point is driven over the surge line.

### 4.2 Simulation of active surge stabilization

Simulations of the proposed active surge control approach will now be presented. The idea is to control the compressor speed with feedback from the mass flow so that the compressor can operate in a stable mode even to the left of the surge line and thereby avoiding

the unstable operation demonstrated in the simulations above.

The controller is implemented with the input torque given by (21), with a desired shaft speed of  $\omega_d = 400/s = 24000 \text{ rpm}$ . In this simulation, the controller is active at all times, and as the same mass flow drop as in the surge simulation above is introduced at  $t = 5 \text{ s}$ , the compressor remains stable. This can be seen in Figure 9, where the mass flow, pressure rise, shaft speed and drive torque are plotted as a function of time. The mass flow is reduced from  $4.9 \text{ kg/s}$  to  $4.2 \text{ kg/s}$ , a value that in open loop would cause the compressor to surge. In this controlled case it remains stable. The peak in the applied torque from the drive as seen in the lower left plot of Figure 9 is expected to be within the performance envelope of the drive. The reason for the slightly increased speed as the torque is reduced is that the compressor torque is reduced with reduced mass flow as can be seen from equation (4). From simulations it is found that the speed control by using drive torque has quite good performance. As can be seen from Figures 9 and 10, the desired speed of  $24000 \text{ rpm}$  is not quite reached. This deviation lies within the small region around the equilibrium, as concluded in section 3.2. As can be seen in Figure 10, the new stable operating point is located to the left of the surge line, illustrating the capability of the control system to achieve active surge control.

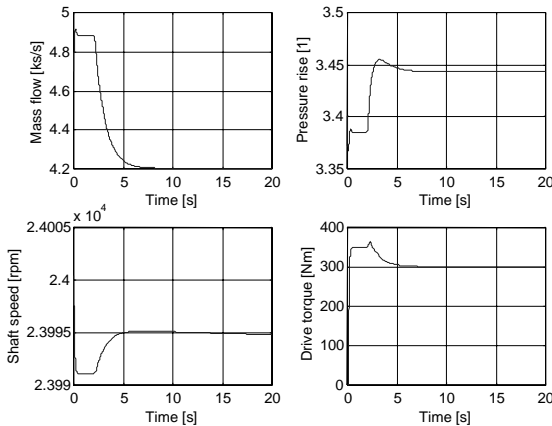


Figure 9: Active surge control using drive torque.

## 5 Conclusion

Active surge controllers for a centrifugal compressor driven by an electrical motor have been designed. This is a new approach to the active surge control problem. The use of the rotational speed as control variable renders the equilibrium globally exponentially stable, and the use of the drive torque as control ensures exponential convergence. The control manipulates the compressor map in such a way that the compressor sees a negative compressor characteristic slope even to the left of the surge line. Simulations confirmed the theory.

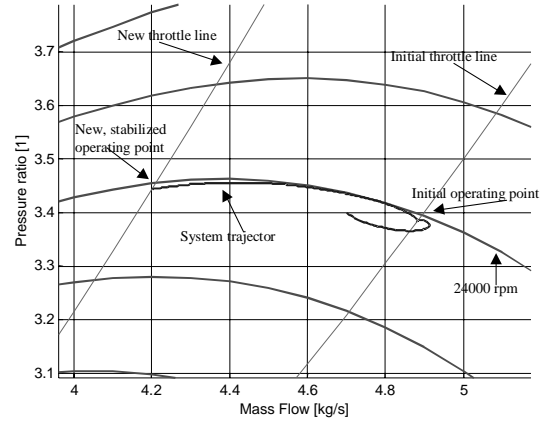


Figure 10: The simulation plotted in the compressor map.

## References

- [1] A. Epstein, J. F. Williams, and E. Greitzer, "Active suppression of aerodynamic instabilities in turbomachines," *Journal of Propulsion and Power*, vol. 5, no. 2, pp. 204–211, 1989.
- [2] J. Gravdahl and O. Egeland, *Compressor surge and rotating stall: modeling and control*. Advances in Industrial Control, London: Springer-Verlag, 1999.
- [3] F. Willems and B. de Jager, "Modeling and control of compressor flow instabilities," *IEEE Control systems*, vol. 19, no. 5, pp. 8–18, 1999.
- [4] E. Greitzer, "Surge and Rotating stall in axial flow compressors, Part I: Theoretical compression system model," *Journal of Engineering for Power*, vol. 98, pp. 190–198, 1976.
- [5] D. Fink, N. Cumpsty, and E. Greitzer, "Surge dynamics in a free-spool centrifugal compressor system," *Journal of Turbomachinery*, vol. 114, pp. 321–332, 1992.
- [6] J. Gravdahl and O. Egeland, "Centrifugal compressor surge and speed control," *IEEE Transactions on Control Systems Technology*, vol. 7, no. 5, 1999.
- [7] J. Gravdahl, F. Willems, B. de Jager, and O. Egeland, "Modeling for surge control of centrifugal compressors: Comparison with experiment," in *Proceedings of the 39th IEEE Conference on Decision and Control*, (Sydney, Australia), 2000.
- [8] J. Gravdahl, F. Willems, B. de Jager, and O. Egeland, "Modeling for surge control of centrifugal compressors: Experimental validation." Submitted to *IEEE Transactions on control systems technology*, 2000.
- [9] A. Whitfield and N. Baines, *Design of Radial Turbomachines*. Harlow: Longman, 1990.
- [10] F. Willems, *Modeling and Bounded Feedback Stabilization of Centrifugal Compressor Surge*. PhD thesis, Fac. of Mechanical Engineering, Eindhoven University of Technology, 2000.
- [11] J. Simon and L. Valavani, "A Lyapunov based nonlinear control scheme for stabilizing a basic compression system using a close-coupled control valve," in *Proceedings of the 1991 American Control Conference*, pp. 2398–2406, 1991.